Journal of Electrical and Electronics Engineering (IOSR-JEEE)
e-ISSN: 2278-1676, p-ISSN: 2320-3331, Volume 20, Issue 4 Ser. 1 (July. – August. 2025), PP 11-21
www.iosrjournals.org

Component Based Modeling And H-Infinity Controlled Hybrid Solar - Gas Turbine For Environmentally Friendly Power Generating System

M. U. Anyaehie[1], E. N. C. Okafor[2], D. O. Dike[3], L. O.Uzoechi[4], N. Chukwuchekwa[5], I. O. Akwukwaegbu[6]
(Electrical/Electronic Engineering Department, Federal Polytechnic Nekede Owerri, Nigeria)
(Electrical Engineering Department, Federal University Of Technology Owerri, Nigeria)

Abstract:
Background*: Achieving a sustainable and environmentally friendly power generating system has become a major challenge in both the public and private sectors of developing nations. Several effort has been put in place and painstaking research had been done in various institutions and laboratories for solutions to this mind bouging issue of inadequate power supply and environmental degradation occasioned by the continious release of green-house gas into the atmosphere. Most institutions of higher learning as well as public and private enterprises in Nigeria are faced with the issue of inadequate power supply from the public utility source and this had made them to resort to standby power generating sources for the their daily operation. This paper presents the integration of renewable energy source (solar) with a gas turbine running as a hybrid system to generate electricity.*
Materials and Methods*: Component-based modeling methodology was adopted to model the various components that makes up the hybrid system and implemented the modeled feedback controlled system using H-infinity Synthesis.*
Results*: The MATLAB® simulated result showed that the H-infinity controlled hybrid power system addressed the problems of reliability and sustainability by reducing the settling time of the hybrid power system to 0.84seconds which represents 94% improvement of the hybrid system performance such that it can perform optimally even in the presence of significant disturbances.*
Conclusion: *The paper concluded by stating that these characteristics will guarantee robust performance for a hybrid power system needed for a sustainable and environmentally friendly power generation.*
Key Word*: Solar energy, Hybrid, Generation, Model, Renewable, Central receiver, Gas turbine.*

Date of Submission: 19-07-2025 Date of Acceptance: 29-07-2025

I. Introduction

Inadequate and unreliable power supply system has become a major challenge to most developing countries with its associated setbacks. To improve on this problem, most educational institutions, public and private organizations, ministries, departments and agencies of have resorted to private generating units as an alternative. The proliferation of these standby generators which mostly runs on fossil fuel has thus created its own problems ranging from noise pollution to environmental degradation occasioned by the release of green-house gases (GHG) and the high running cost for fuelling, servicing and maintenance of these standby generators[1,2]. The hybrid renewable energy system (HRES) is therefore one of the ways of addressing issues arising from fossil fuel combustion which has become a major global challenge. A hybrid system is usually made up of more than one type of energy sources. It can be a combination of a diesel powered generator with any other source of energy such as tidal wave, solar, wind, or geothermal[3,4]. Solar energy can be considered as the most efficient, available, reliable and economic source for any hybridization scheme. It is environmentally friendly, unlike fossil fuel[5]. This is due to the ease of harnessing solar thermal energy by suitable conversion techniques. Direct Normal Insolation (DNI) can be obtained by means of beam radiation which uses fraction of sunlight that are not deviated by atmospheric agents.

The average daily solar radiation on horizontal surface across Nigeria is within the range of 4.5 $kW.hr/m^2$ in the southern parts to 6.6 $kW.hr/m^2$ northwards. Using the average daily solar radiation of the entire country, which is 6 $kW.hr/m^2$ about 5545×10^3 $MW.hr$ electric energy can be received from solar radiation on daily basis[6,7]. With this high potential of solar energy, substantial amount of electricity can be generated by the process of integrating this renewable source into a conventional generator (turbine) to achieve an environmental friendly and cost effective power generation through the process of hybridization.

Whereas the poor and unreliable power supply from some of the electricity service providers or distribution network operators (DNO) has made most residential, commercial and industrial facilities to run on stand-by generators, there is no adequate compensation or robust control system to enable these generating plants to withstand significant disturbances. System robustness had become a very important area of research due to the high level of system performance optimization and stability achieved when adequately implemented. Robust control technique deals clearly with system uncertainties in its approach to controller design, aiming to achieve robust performance and stability in the presence of modeling errors and disturbances[8]. System controllers designed using robust control methods tend to have the ability to cope with the disturbances or imbalances in the system in order to ensure the system stability and maintain system optimal performance. Some of the examples of modern robust control techniques include H-infinity loop-shaping, Sliding Mode Control (SMC) and artificial intelligence (AI) based control such as Artificial Neural Network (ANN), Fuzzy Logic Control (FLC). Other techniques of robust controller design are discussed in[9,10,11,12,13,14].

II. Material And Methods

The component based modeling technique involves the development of the mathematical submodels of the individual components that makes up the complete system. This comprises of the solar central receiver system (CRS) and the conventional synchronous generator while the hybridization scheme involves the combination of the two sources to power the gas turbine[15]. The dynamic model of the solar thermal system subunits consisting of: refocus, receiver, governor and turbine will be presented. This will be followed by the synchronous generator model. The performance of the hybrid system will be monitored and thereafter improved by introducing a system controller based on the H-infinity loop shaping technique. This will require the generation of H-infinity synthesis control algorithm to carry out the complex computations and iterations of robust controller design in MATLAB. The open loop gain graph (L), sensitivity graph (S) and closed loop gain graph (T) also known as complementary sensitivity graph will be plotted to check the overall performance, sustainability and stability of the controlled system.

Solar Central Receiver System

Figure 1 shows the different types and categories of solar collectors which are divided into the concentrating and non- concentrating collectors. In the concentrating type solar collector, various types of mirrors, reflectors or concentrators are used to concentrate the solar energy and they provide higher temperatures (i.e., 400–1000ºC) than non-concentrating type collectors[16]. Hence, the concentrating collectors are selected for this paper based on its advantages and ease of adaptation and integration into a central receiver system shown in figure 2.

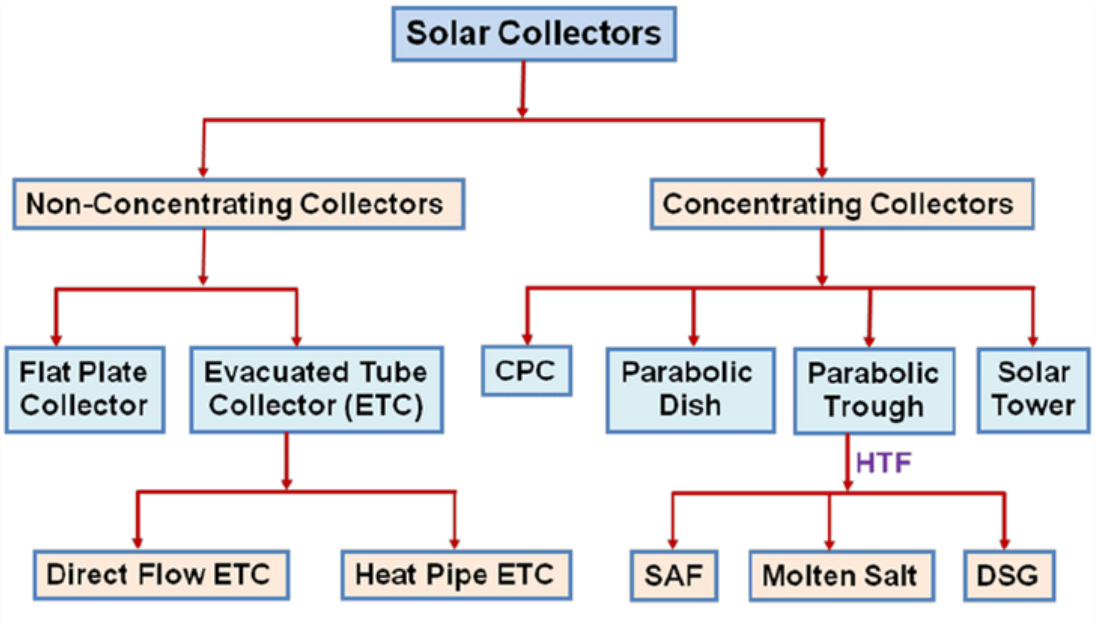

Figure 1: Types and categories of solar collectors[16].

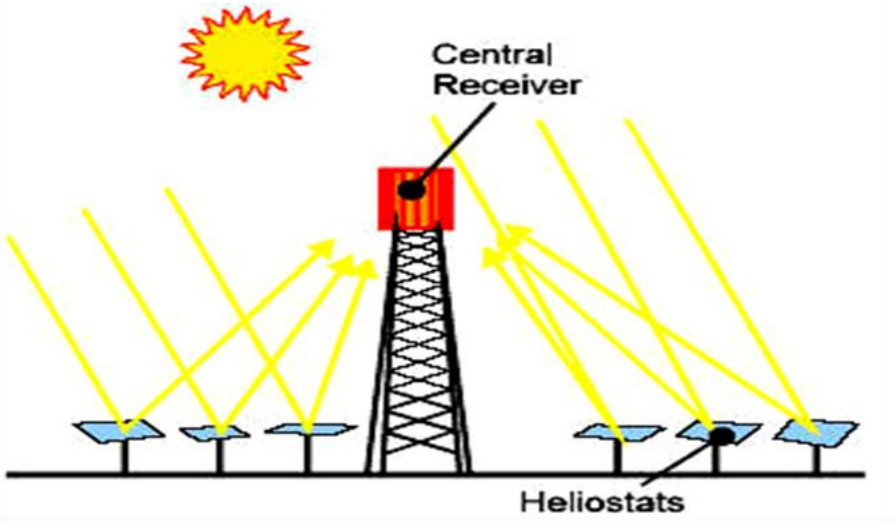

Figure 2: Central receiver solar system[17].

Operation of Gas Turbines

Gas turbines are made up of three primary sections mounted on the same shaft: the compressor, the combustion chamber (or combustor) and the turbine as shown in figure 3. The compressor can be either axial flow or centrifugal flow. Axial flow compressors are more common in power generation because they have higher flow rates and efficiencies. They are comprised of multiple stages of rotating and stationary blades (or stators) through which air is drawn in parallel to the axis of rotation and incrementally compressed as it passes through each stage.

The acceleration of the air through the rotating blades and diffusion by the stators increases the pressure and reduces the volume of the air.

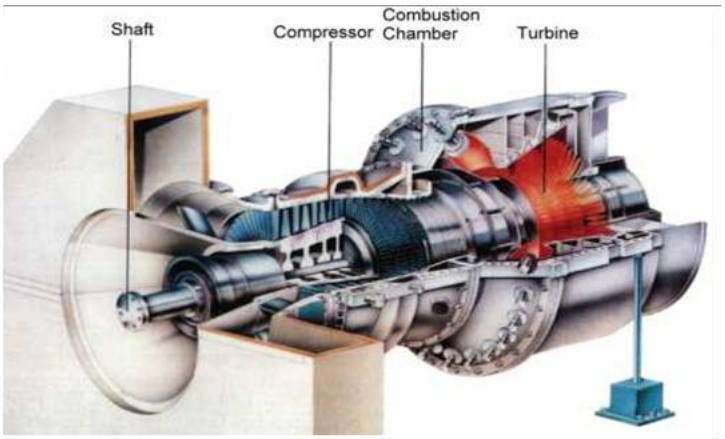

Figure 3: Sectional view of a typical gas turbine[18].

In an ideal gas turbine, the working fluid (gases) undergoes four thermodynamic processes. These includes: compression at constant temperature, combustion at constant pressure, expansion at constant temperature and heat rejection. Together, these processes make up the Brayton cycle. Solar – gas turbines are those that operate from a working fluid whose operational/turbine inlet temperatures are obtained through direct concentration of thermal or heat energy from the sun. These can be achieved by using either solar concentrators or parabolic reflectors.

The hybrid Solar – Gas Turbine

The schematic layout of the proposed hybrid solar gas-turbine is presented in figure 4. The figure shows the major constituents of the system which will be modeled on component basis. This figure can be translated into the block diagram as given in figure 5.

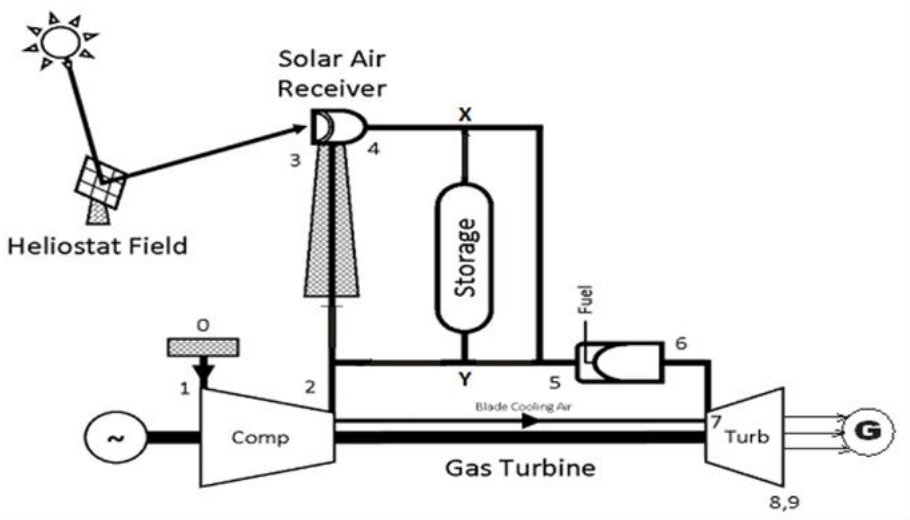

Figure 4: Schematic Layout a typical hybrid solar gas-turbine with storage device[19].

The items labeled V1 toV6 are the various control valves, which regulates the operation of the system. The hybrid system consists mainly of the solar thermal system unit and the conventional synchronous generator unit as major inputs into the combustion chamber. This is presented in figure 6 as constituents of the hybrid system model.

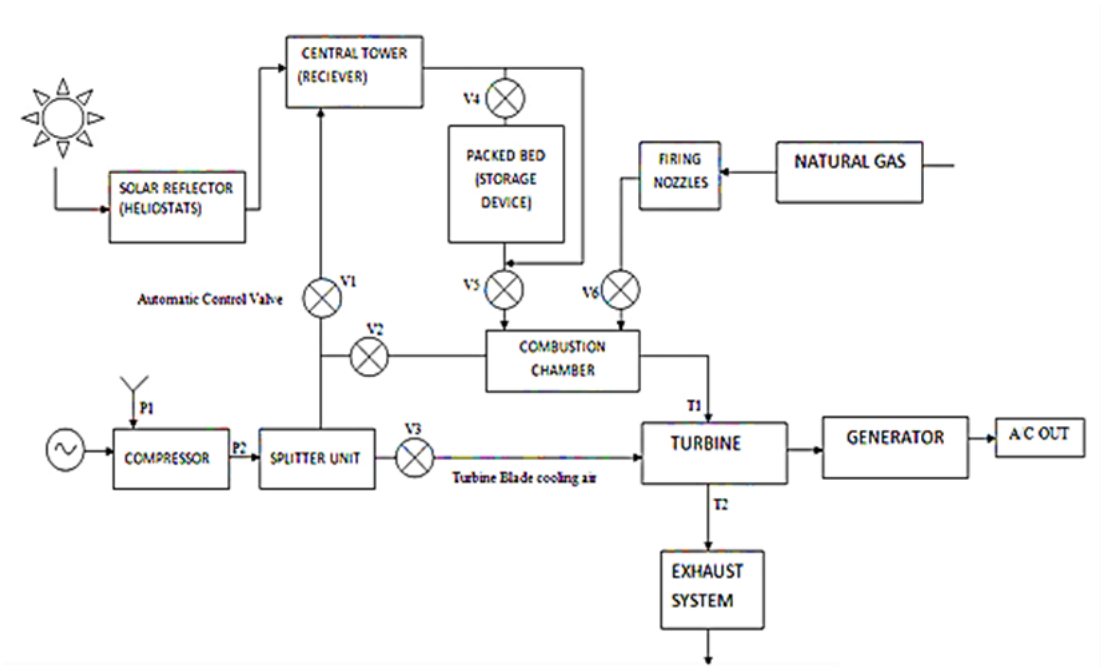

Figure 5: Block diagram of the Proposed Hybrid System

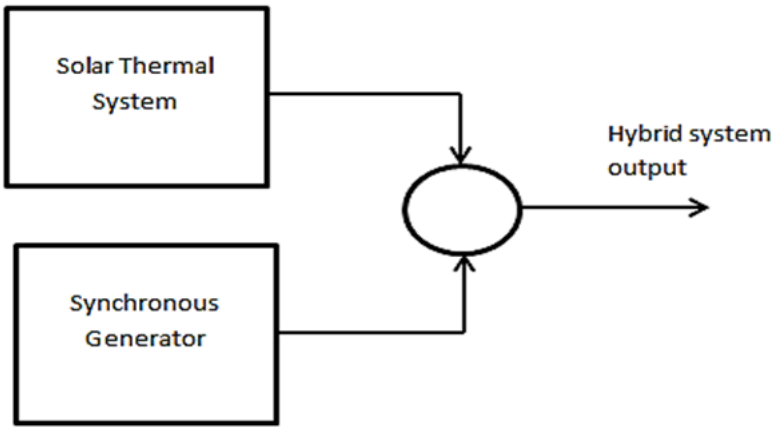

Figure 6: Hybrid system model

The performance behavior of this system can be determined by component-based modeling of the various constituent units of the system.

Solar Thermal System Component Model

The solar thermal system also known as central receiver solar thermal system consists of four subunits connected together. The subunits are: The refocus, receiver, governor and turbine.

The component model of the solar thermal system subunits dynamics are illustrated as follows:

The refocus dynamic model is given as:

$$G_{RF} = \frac{K_{RF}}{1+sT_{RF}} \quad (1)$$

The receiver dynamic model is given as:

$$G_{RV} = \frac{K_{RV}}{1+sT_{RV}} \quad (2)$$

The governor dynamic model is given as:

$$G_G = \frac{K_G}{1+sT_G} \quad (3)$$

The turbine dynamic model is given as:

$$G_T = \frac{K_T}{1+sT_T} \quad (4)$$

The Central Receiver Solar Thermal System (CRSTS) component model becomes:

$$G_{CRSTS} = \left(\frac{K_{RF}}{1+sT_{RF}}\right)\left(\frac{K_{RV}}{1+sT_{RV}}\right)\left(\frac{K_G}{1+sT_G}\right)\left(\frac{K_T}{1+sT_T}\right) \quad (5)$$

Where:

K_{RF} is the gain of refocus, T_{RF} is the time constant of refocus,
K_{RV} is the gain of receiver, T_{RV} is the time constant of the receiver,
K_G is the gain of governor, T_G is the time constant of the governor,
K_T is the gain of turbine, T_T is the time constant of the turbine,

Conventional Synchronous Generator Component Model

The synchronous generator model used here consists of three subunits, namely the governor, turbine and load/machine, and the transfer function component models are presented as follows:

The governor dynamic model is given as:

$$G_g(s) = \frac{1}{T_{G1}s+1} \quad (6)$$

The turbine dynamic model is given as:

$$G_t(s) = \frac{1}{T_{T1}s+1} \quad (7)$$

The load and Machine dynamic model is given as:

$$G_p(s) = \frac{K_p}{T_p s+1} \quad (8)$$

The Conventional Synchronous Generator (CSG) component model becomes:

$$G_{CSG}(s) = \left(\frac{1}{T_{G1}s+1}\right)\left(\frac{1}{T_{T1}s+1}\right)\left(\frac{K_p}{T_p s+1}\right) \quad (9)$$

Where:

T_{G1} is the time constant of the synchronous generator governor
T_{T1} is the time constant of the synchronous generator turbine
T_p is the overall conventional system time constant
K_p is the overall conventional system gain

The Hybrid System Model Presentation

The hybrid system model as illustrated in figure 6 which comprises of the solar thermal system and the

conventional synchronous generator system is presented as follows:

$$G_{HS}(s) = G_{CRSTS} + G_{CSG}(s) \quad (10)$$

This becomes:

$$G_{HS}(s) = \left(\frac{K_{RF}}{1+sT_{RF}}\right)\left(\frac{K_{RV}}{1+sT_{RV}}\right)\left(\frac{K_G}{1+sT_G}\right)\left(\frac{K_T}{1+sT_T}\right) + \left(\frac{1}{T_{G1}s+1}\right)\left(\frac{1}{T_{T1}s+1}\right)\left(\frac{1}{T_ps+1}\right) \quad (11)$$

The system dynamic model parameters are presented in table 1.

Table no 1: Shows System dynamic model parameters [20].

S/N	Parameter	Value
1	Gain of refocus, K_{RF}	1
2	Gain of receiver, K_{RV}	1
3	Gain of governor, K_G	1
4	Gain of turbine, K_T	1
5	Time constant of refocus, T_{RF}	1.33s
6	Time constant of the receiver, T_{RV}	4s
7	Time constant of the governor, T_G	0.08s
8	Time constant of the turbine, T_T	1s
9	Gain of the synchronous generator, T_{G1}	0.08
10	Delay of the synchronous generator, T_{T1}	0.3s
11	Overall conventional system gain, K_p	1
12	Overall conventional system time constant, T_p	0.08s

Development of a Robust Control Performance Improvement and Stability of the Hybrid System Using H-Infinity Technique.

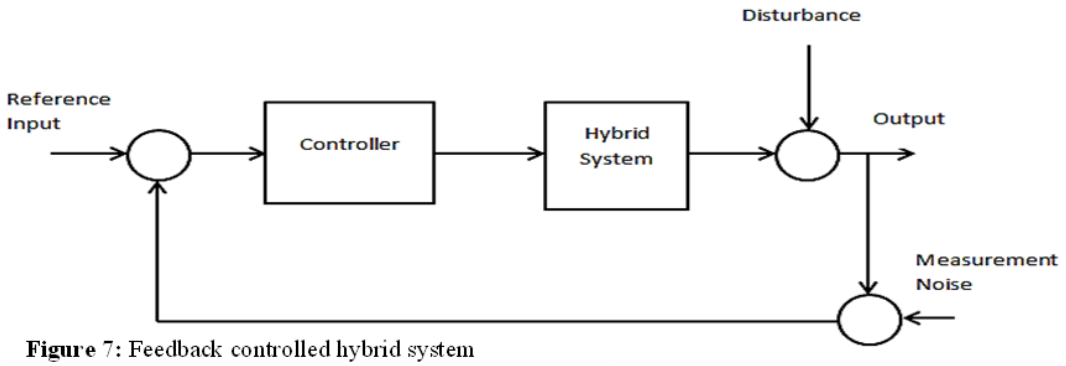

Figure 7: Feedback controlled hybrid system

Having carried out the complete modeling of the individual components of the system and presented the dynamic model of the hybrid system, there is the need to develop a control system to improve the performance and stability of the system. This is achieved by introducing a feedback control system using hybrid infinity technique. The block diagram of the improved system is given in figure 7. The result of this improved system and its analysis is presented subsequently.

The state space model representation of the developed control system K for the solar energy based hybrid system is given as follows:

$$\begin{aligned} \dot{x} &= Ax + Bu \\ y &= Cx + Du \end{aligned} \quad (12)$$

The first part of the equation is the state equation while the second part is the output equation. Where, x and $\dot{x}$ are the state vector and the differential state vector respectively, u and y are input vector and output vector respectively.

A is the system matrix, B and C are the input and the output matrices respectively, D is the feed-forward matrix, K is the controller in state space with the following states:

$$A = \begin{bmatrix} -688.2 & -1307 & -2241 & -2565 & -2203 & -1330 & 765.2 & 4992 \\ 32 & 0 & 0 & 0 & 0 & 0 & 0 & 0 \\ 0 & 16 & 0 & 0 & 0 & 0 & 0 & 0 \\ 0 & 0 & 8 & 0 & 0 & 0 & 0 & 0 \\ 0 & 0 & 0 & 2 & 0 & 0 & 0 & 0 \\ 0 & 0 & 0 & 0 & 1 & 0 & 0 & 0 \\ 0 & 0 & 0 & 0 & 0 & 0.5 & 0 & 0 \\ 0 & 0 & -2.22e-16 & -4.441e-16 & 0 & 0 & -1.11e-16 & -0.01 \end{bmatrix}$$

$$B = \begin{bmatrix} 0 \\ 0 \\ 0 \\ 0 \\ 0 \\ 0 \\ 0 \\ 1.056 \end{bmatrix}$$

$$C = [-611.2 \quad -1217 \quad -2114 \quad -2426 \quad -2084 \quad -1258 \quad -724.4 \quad 4727]$$

$$D = [0]$$

III. Result

The Central Receiver Solar Thermal System (CRSTS) and Conventional Synchronous Generator System Performance and Stability Analysis.

The simulation result for the transfer function of the CRSTS component model is given in equation (13). The step response of the system is shown in figure 8a while figure 8b gives the Bode plot for the CRSTS stability analysis

$$G_{CRSTS} = \frac{1}{0.4256s^4+6.172s^3+11.16s^2+6.41s+1} \quad (13)$$

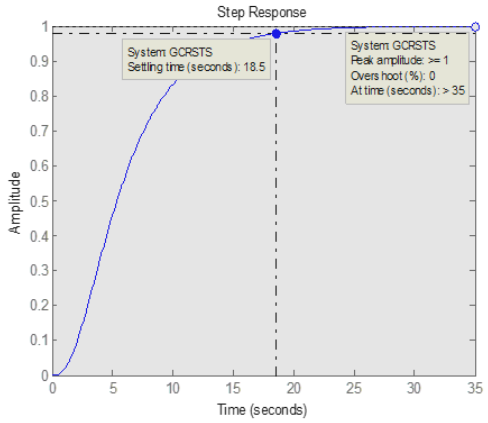

Figure 8a: Step response of the solar thermal system

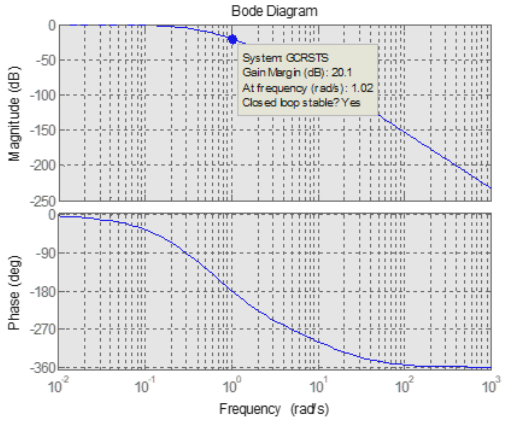

Figure 8b: CRSTS stability analysis

The Conventional Synchronous Generator simulation transfer function is given in equation (14) while the system Performance and Stability Analysis is given in figure 9.

$$G_{CSG} = \frac{1}{0.00192s^3+0.0544s^2+0.46S+1} \quad (14)$$

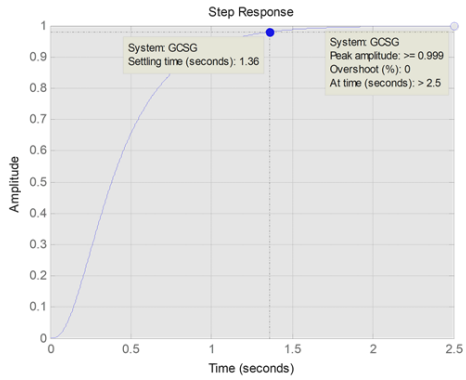

Figure 9a: CSG step response

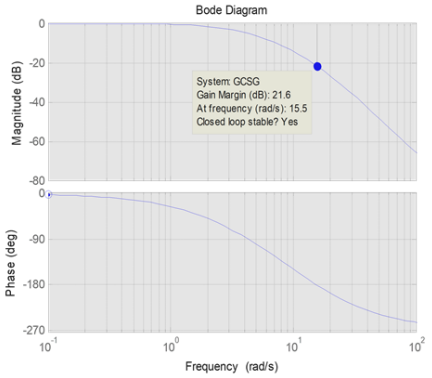

Figure 9b: CSG stability analysis

Hybrid System (HS) Performance and Stability Analysis

The transfer function simulation result of the hybrid system is given in equation (15) while figures 10a and 10b gives the hybrid system step response and stability analysis respectively.

$$G_{HS} = \frac{0.4256s^4+6.174s^3+11.21s^2+6.87s+2}{0.0008s^7+0.04s^6+0.55s^5+3.88s^4+1165s^3+14.16s^2+6.87s+1} \quad (15)$$

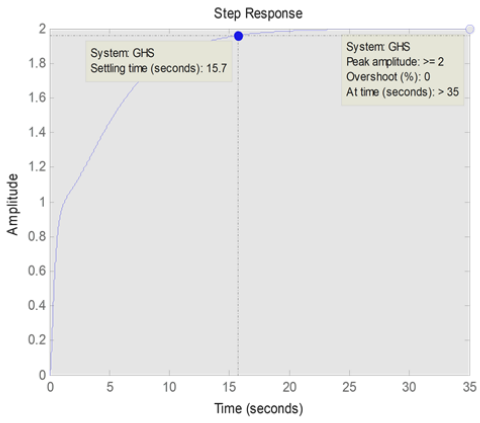

Figure 10a: Hybrid system step response

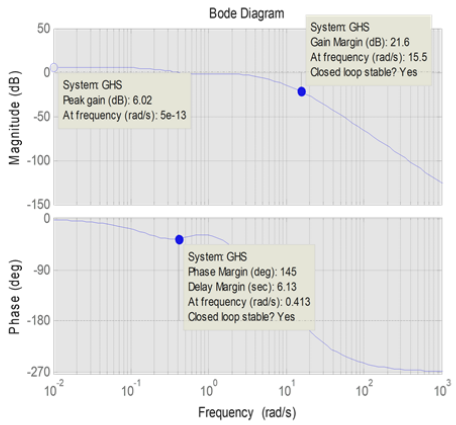

Figure 10b: Hybrid system stability analysis

H-infinity Controlled Hybrid System Performance and Stability Analysis

Figure 11a shows the performance behavior of the controlled system for the development of the controller through loop shaping. This comprises the open loop gain graph (L), sensitivity graph (S) and closed loop gain graph (T) also known as complementary sensitivity graph.

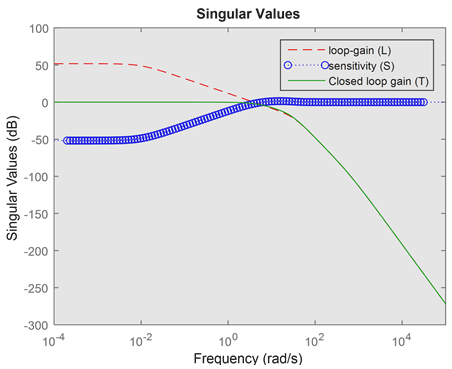

Figure 11a: Sigma plot of the controlled hybrid System

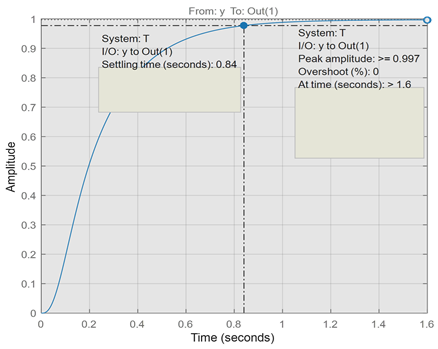

Figure 11b: System Step response

The controlled system recorded open loop gain a bit higher than 50dB magnitude which shows good level of gain. The closed loop graph determines the system trajectory tracking which shows the level of error in the design and also it shows how close the actual output is to the desired output. From the result, the closed loop graph tracked the 0dB line which shows that the error was cancelled very well during the design. The sensitivity graph determines the disturbance rejection ability of the controlled system. Disturbance is a low frequency issue; therefore to address it, the sensitivity graph must be very much lower than 0dB at low frequencies. From the results, the sensitivity graph recorded about -50dB which shows that the system achieved good disturbance rejection characteristics.

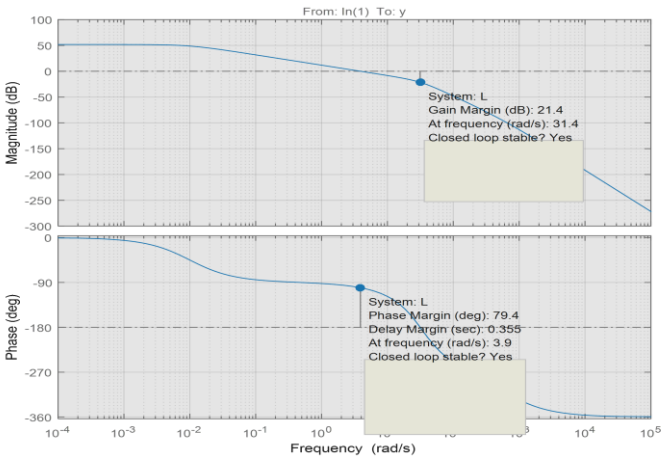

Figure 12: Bode plot of the controlled hybrid system

IV. Discussion

The results in figures 8a and 8b show that the central receiver solar thermal system:

i. Recorded a 0% overshoot which is very good.
ii. Recorded settling time of 18.5 seconds which is very high.

This means that it takes 18.5 seconds to come back to its equilibrium level or normal performance after occurrence of disturbance.

The results in figure 10a and 10b show that:

i. The hybrid system recorded a 0% overshoot which is very good.
ii. The hybrid system also recorded settling time of 15.7 seconds which is very high.

This means that it takes 15.7 seconds to settle back to its equilibrium level or normal performance after occurrence of disturbance. Such amount of time is so significant that the system will not perform satisfactorily because it may cause some damages when there is disturbance or surge due to lightening, short circuiting, or other types of faults. Since there are a lot of disturbances and measurement noise in the power system and other uncertainties due to unmodelled dynamics etc., therefore the system settling time should be reduced to possibly less than 1second to enable the system perform better.

The results in figure 11b show the step response of the controlled hybrid power system performance. This indicates the time it takes the system to return to equilibrium or normal performance level after encountering disturbance. It also represents the time it takes the system to cancel the effects of disturbance or faults in the system.

The Bode plot for the stability analysis of the controlled hybrid system is given in figure 12.

From the results, the controlled system recorded 0.84 seconds settling time which is a significant improvement over the 15.7 seconds recorded by the hybrid system without the developed controller. The open loop gain must be very much higher than 0dB for a good design while maintaining gain margin greater than or equal to 20dB and phase margin greater than or equal to 60 degrees. These characteristics were satisfied in the Bode plot shown in figure 12.

Computing the percentage difference in the settling time improvement:

15.7- 0.84 = 14.86
14.86/15.7 = 0.9464
0.9464 x 100 = 94.64%

Therefore, the component based model and H-infinity controlled hybrid solar gas – turbine power system achieved 94.64% improvement in settling time.

V. Conclusion

The component based method of the hybrid system modeling comprised of the solar thermal system and the conventional generator. From the existing system analysis, the solar thermal system recorded a 0% overshoot which is very good. The solar thermal system recorded settling time of 18.5 seconds which is very high. This means that it takes 18.5 seconds to come back to its equilibrium level or normal performance after occurrence of disturbance. Such characteristic will not allow the system to perform so well when faults occur especially in places where there is likely to be many contributing factors to faults such as overloading, generator trip, etc. The hybrid system recorded overshoot of 0% which is very good. The hybrid system also recorded settling time of 15.7 seconds which is very high. This means that it takes 15.7 seconds to settle back to its equilibrium level or normal performance after occurrence of disturbance. Such amount of time is so significant that the system will not perform satisfactorily because it may cause some damages when there is disturbance or surge due to lightning, short circuiting, or other types of faults. Since there are a lot of disturbances and measurement noise in the power system and other uncertainties due to unmodelled dynamics, etc., especially in the developing country such as Nigeria, therefore the system settling time should be reduced to possibly less than 1second to enable the system perform better. Reducing the system settling time will result to achieving a faster system which can retain its equilibrium seamlessly after occurrence of disturbance. Hence, there is need for a robust control technique.

H-infinity synthesis robust control technique was introduced to the hybrid system to improve the performance and stability of the system. The performance behavior of the controlled system for the development of the controller through loop shaping was improved. This comprises the open loop gain graph, sensitivity graph and closed loop gain graph also known as complementary sensitivity graph. The controlled system recorded open loop gain a bit higher than 50dB magnitude which shows good level of gain. The closed loop graph determines the system trajectory tracking which shows the level of error in the design and also it shows how close the actual output is to the desired output. From the result, the closed loop graph tracked the 0dB line which shows that the error was cancelled very well during the design. The sensitivity graph determines the disturbance rejection ability of the controlled system. Disturbance is a low frequency issue, therefore to address it the sensitivity graph must be very much lower than 0dB at low frequencies. From the results, the sensitivity graph recorded about -50dB which shows that the system achieved good disturbance rejection characteristics. Thus the controlled hybrid power system achieved 94.64% improvement in settling time over the uncontrolled hybrid power system. The open loop gain, which must be very much higher than 0dB for a good design while maintaining gain margin greater than or equal to 20dB and phase margin greater than or equal to 60 degrees was achieved.

It can be concluded that the H-infinity controlled hybrid solar thermal and conventional generator power system achieved improved performance and stability with reduced settling time of 0.84seconds, overshoot of 0% with gain margin greater than 20dB and phase margin greater than 60deg. These characteristics will guarantee a robust performance for the hybrid power system to power institutions complex power line network, large covering area and heavy loads such as is needed for sustainable and environmentally friendly power generating system.

References

[1]. Anyaehie M. U. "Power & Energy And National Development", 2nd Annual Conference Journal Of School Of Business & Management Technology (SBMT), Federal Polytechnic Nekede, Nigeria. 2009;1(1):146-154.

[2]. Manzoore, E. M., Soudagar, S. S., Deepali, M., Pramod, B., Mohammad, Nur-E-Alam, Tiong, S. K., Ramesh, S., Armin, R., Harish, V., Yunus, K. T. M, Mujtaba, M. A., Kiran, S., Kalam, M. A., Fattah, I.M.R. Optimizing IC Engine Efficiency: A Comprehensive Review On Biodiesel, Nanofluid, And The Role Of Artificial Intelligence And Machine Learning, Energy Conversion And Management, 2024;307: 118337,

[3]. Deshmukh, M. K. And Deshmukh, S. S. Modeling Of Hybrid Renewable Energy Systems. Renewable And Sustainable Energy Reviews, Elsevier Ltd, 2008; 12: 235–249.

[4]. Abshishek, R. Introduction To ANN (Artificial Neural Networks) Set 3 (Hybrid Systems) Www.Geeksforgeeks.Org/Introduction-Ann-Artificial-Neural-Networks-Set-3-Hybrid-Systems/#Article-Meta-Div, Accessed On July 14, 2023

[5]. Ntekim, B. E., And Uppin, C. "Optimization And Modeling Of Solar Energy With Artificial Neural Networks", Nigerian Journal Of Technology, 2024;43(7)131 –138; Https://Doi.Org/10.4314/Njt.V43i1.15

[6]. Boyi, J., Jibril, Y., And Mu'azu, M. B. Solar Radiation Characteristics And Potential As Renewable Energy Source In Nigeria, The 22nd Nigerian Society Of Engineers, Electrical Division, International Conference Proceedings 2006, Pp. 33-35.

[7]. Iwuamadi, O. C., Anyaehie, M. U. And Nwadike S. U. Design Specifications Of A 5.56MW Solar Photovoltaic Power Plant In Federal Polytechnic Nekede, Owerri, Nigeria, Global Scientific Journals (GSJ), 2022;10(7):1470-1476.

[8]. Agbaraji, C. E. "Robustness Analysis Of A Closed-Loop Controller For A Robot Manipulator In Real Environments", Physical Science International Journal, 2015;8(3):1-11.

[9]. Bala, G. Robust Control Toolbox, Getting Started Guide, Mathworks Inc. USA, 2013.

[10] Gu, D.W. Robust Control Design With Matlab, Springer-Verlag Limited London, 2005.

[11]. Kemin, Z. Essentials Of Robust Control, Prentice Hall, New Jersey, 1999.
[12]. Popescu, D. Analysis And Synthesis Of Robust Systems, Universitatea Publishing House, Craiova, Romania, 2010.
[13]. Sename, O. Robust Control Of MIMO Systems, GIPSA-Lab Surface Meteorological And Solar Energy Data Table, NASA, 2013.
[14]. Dulau, M. And Bica, D. Design Of Robust Control For Single Machine Infinite Bus System, Procedia Technology, 2015;(19): 657-664,.
[15]. Olivenza-León, D., Medina, A., And Calvo, H. A. Thermodynamic Modeling Of A Hybrid Solar Gas-Turbine Power Plant, ELSEVIER Energy Conversion And Management Journal 2015;(93): 435–447.
[16]. Nagarajan, S., Barshilia, H., And Rajam, K. Review Of Sputter Deposited Mid- To High - Temperature Solar Selective Coatings For Flat Plate/Evacuated Tube Collectors And Solar Thermal Power Generation Applications, Www.Researchgate.Net/Publication/277327602_, Accessed On March, 22 2020.
[17]. Arslan, A. R., Syed, N. D., Abdelrahman, El-Leathy., Hany, Al-Ansary., Dong, Y. A Review And Classification Of Layouts And Optimization Techniques Used In Design Of Heliostat Fields In Solar Central Receiver Systems, Elsevier Solar Energy, 2021;218:296-311
[18]. Lemma, T. A., And Hashim, F. Wavelet Analysis And Auto-Associative Neural Network Based Fault Detection And Diagnosis In An Industrial Gas Turbine. BEIAC 2012 – 2012 IEEE Business, Engineering And Industrial Applications Colloquium, 10.1109/BEIAC.2012.6226031:103-108.
[19]. Fricker, H., Regenerative Thermal Storage In Atmospheric Air System Solar Power Plant, Energy Systems, 2004;29:871-881.
[20]. Latif, A., Das, D. C., Barik, A. K., Ranjan, S. Maiden Co-Ordinated Load Frequency Control Strategy For ST-AWEC-GEC-BDDG Based Independent Three-Area Interconnected Microgrid System With Combined Effect Of Diverse Energy Storage And DC Link Using BOA Optimized PFOID Controller IET Review. Power Generation, 2019;10:2634-2646.